THE AMERICAN SOCIETY OF MECHANICAL ENGINEERS
Three Park Avenue, New York, N.Y. 10016-5990

99-GT-113

DETAILED ANALYSIS OF THE ACOUSTIC MODE SHAPES OF AN ANNULAR COMBUSTION CHAMBER

Günther Walz, Werner Krebs, Stefan Hoffmann and Hans Judith

SIEMENS AG KWU, 45466 Mülheim a.d. Ruhr

Abstract

To get a better understanding of the formation of thermoacoustic oscillations in an annular gasturbine combustor, an analysis of the acoustic eigenmodes has been conducted using the Finite Element (FE) method. The influence of different boundary conditions and a space dependent velocity of sound has been investigated. The boundary conditions actually define the eigenfrequency spectrum. Hence, it is crucial to know e.g. the burner impedance. In case of the combustion system without significant mixing air addition considered in this paper, the space dependence of the velocity of sound is of minor importance for the eigenfrequency spectrum leading to a maximum deviation of only 5% in the eigenvalues.

It is demonstrated that the efficiency of the numerical eigenvalue analysis can be improved by making use of symmetry, by splitting the problem into several steps with alternate boundaries conditions, and by choosing the shift frequency ω_s in the range of frequencies one is interested in.

Notation

c	speed of sound
L	Axial length of the cylindrically shaped combustor
N	discrete integer values to characterise the individual eigenmodes
(nlmk)	set of integer values N to characterise the eigenmodes of the cylindrically shaped combustor
p	acoustic pressure
r_a	outer radius of the cylindrically shaped combustor
r_i	inner radius of the cylindrically shaped combustor
t	time

Presented at the International Gas Turbine & Aeroengine Congress & Exhibition
Indianapolis, Indiana — June 7–June 10, 1999
This paper has been accepted for publication in the Transactions of the ASME
Discussion of it will be accepted at ASME Headquarters until September 30, 1999

V	acoustic velocity
$x=(r,\phi,z)$	spatial coordinates
Φ	scalar velocity potential
Φ_N	eigenfunction corresponding to the eigenfrequency ω_N
κ	compressibility of acoustic medium
ρ	density of acoustic medium
ω_0	eigenfrequency normalising factor (equals the proportionality factor in the limit $N\rightarrow\infty$ according to equation (4))
ω_N	eigenfrequency to be characterised by discrete values of N

1 Introduction

Ring combustors of gasturbines combine the advantages of a reduced requirement for cooling air due to their compact design and a homogeneous temperature distribution upstream of the turbine inlet. Together with lean premixed combustion, this offers the potential of significantly reducing NO_x emissions. Consequently, annular combustion chambers are often applied as a design feature of modern gas turbines such as the Hybrid Burner Ring (HBR-) combustor of the Siemens 3A series [1]. In Fig.1 a cross section of the V84.3A, the 60 Hz version, is shown.

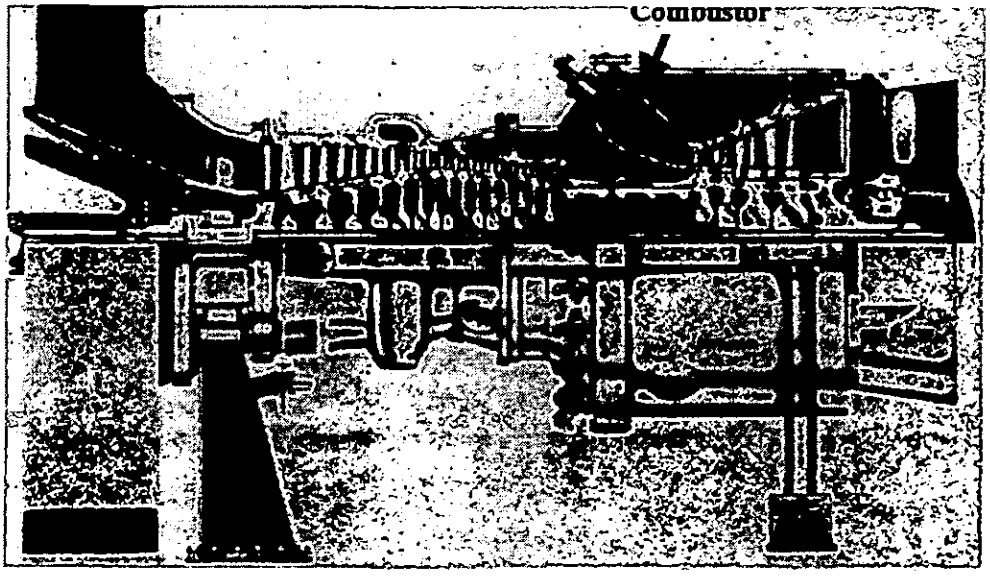

Figure 1: Cross-Section of the V84.3A gasturbine

Due to the ever increasing reaction densities in modern gas turbine combustors, the risk of the formation of thermoacoustic oscillations also rises. These oscillations have been investigated in detail both experimentally and theoretically for single burner arrangements [2], [3]. However, little is known about their mode shapes and excitation in annular combustors. In order to achieve a better understanding of combustion oscillations in annular combustors and to assist the interpretation of dynamic pressure measurements on site, a detailed analysis of the acoustic modes within an annular combustor has been carried out.

The modal analysis has been performed both by application of analytical and Finite Element (FE) tools. In section 2 the essentials of the theory of acoustic wave motion are introduced. The eigenmodes of a cylinder are studied in detail in section 3. Using this simple model the main features of acoustic eigenmodes can be discussed on an

analytical basis. Furthermore, the analytical solution serves as a benchmark for the FE analysis. Since an analytical solution for annular combustion chambers is not available, their eigenmodes are analysed numerically in section 4.

2 Theory

Since the main flow inside gas turbine combustors is characterised by a Mach Number below 0.1, the effect of the mean flow on the transport of acoustic properties can be neglected. Hence, the acoustic wave motion can be determined solving the transport equation for the scalar velocity potential Φ:

$$\frac{\partial^2 \Phi}{\partial t^2} = \frac{1}{k\rho}\Delta\Phi \qquad (1)$$

The fluid is characterised by a compressibility 'k' and density 'ρ' which are assumed to be independent of space for simplicity. Measurable quantities are the acoustic pressure 'p' and the acoustic velocity 'v' which are related to Φ by

$$p = \rho\frac{\partial \Phi}{\partial t}, \quad v = -\,grad\Phi \qquad (2)$$

Both p and v also obey a wave equation of the type (1). The second equation of (2) shown is tantamount to curl v =0 . The speed c of a sound wave is given by

$$c^2 = \frac{1}{k\rho} \qquad (3)$$

Time and space variables are separated by assuming special solutions of the form Φ = A exp(iωt), which are the 'eigensolutions of the Laplacian Δ' at an 'eigenfrequency ω'. On the boundaries of the enclosed region 'V' two conditions can be specified. For an open wall the velocity potential is set to zero (Φ = 0 = p, Dirichlet type for Φ). At a rigid wall, the outer normal component of the acoustic velocity vector v_n is set to zero which means $\partial\Phi/\partial n = 0 = v_n$ (of Neumann type for Φ). With these boundary conditions only discrete values of ω are possible that can be arranged in an ascending order and referenced by an integer N, whereby N is the number of eigenfrequencies smaller than a fixed value ω_N.

It is well-known that there is an infinite number of eigenfrequencies ω_N which are all real and positive (the lowest one =0 for Neumann type boundary conditions). The "higher" eigenfrequencies approach

$$\omega_N \longrightarrow c\left(\frac{N6\pi^2}{V}\right)^{\frac{1}{3}} \equiv N^{\frac{1}{3}}\omega_o \,, \; if\, N \to \infty \qquad (4)$$

In the following the proportionality factor ω_0 which represents a typical value for the eigenfrequencies of the combustor will be used to normalise all eigenfrequencies ω_N . The normalised eigenfrequencies are independent of the speed of sound and the combustor volume, especially in the limit of large N. It is revealed that all frequencies ω_N decrease if the volume is increased and / or the speed of sound is decreased.

The eigenfunctions Φ_N corresponding to different eigenvalues ω_N are orthogonal, i.e.

$$(\Phi_N, \Phi_M) \equiv \int_V \Phi_N \Phi_M \, dV = 0 \quad , N \neq M \qquad (5)$$

They can be selected to form a complete orthonormal set of functions. This means that every solution Φ of the acoustic wave equation (1) can be expanded in terms of the Φ_N:

$$\Phi = \sum_n (\Phi, \Phi_N)\Phi_N \qquad (6)$$

The eigenfunction Φ_1 corresponding to the lowest eigenfrequencies has no nodes (i.e. is non-zero everywhere). If there are J>1 eigenfunctions Φ_J with the same eigenvalue ω_N, the eigenmodes are called J-fold "degenerate". Degeneracy is always related to a type of symmetry.

The set of nodes of Φ_N, for $N \geq 2$, divide the region V into at least two sub-regions and at most, N sub-regions.

In the following chapter, as an example, the eigensolutions of a cylinder with different types of boundary conditions are investigated in detail.

3 Eigenmodes of a cylindrical ring combustion chamber

3.1 Analytical Solution

The geometry of a cylindrical ring is very similar to the annular combustion chamber thus demonstrating the main features of such eigenmodes. The main dimensions are its length L, its outer diameter r_a and its inner diameter r_i. On the other hand the model is simple enough to have an analytical solution available by which it is possible to check the quality of the numerical analysis of the FE method. Assuming rigid walls throughout the entire boundary, the eigenfunctions for cylindrical coordinate system (r,φ,z) can be expressed in the form

$$\phi_{nlm} = Z_n(z) R_{lm}(r) \Psi_m(\varphi) e^{i\omega_{nlm} t} \qquad (7.1)$$

i.e. as a product of an axial contribution $Z_n(z)$, a radial one $R_{lm}(r)$, a circumferential one $\Psi_m(\varphi)$, and of the time dependent factor $\exp(i\omega_{nlm}t)$. The functions Z_n, R_{lm}, and Ψ_m are given by

$$Z_n(z) = \sqrt{\frac{2}{L}} \cos\left(n \frac{\pi}{L} z\right),$$

$$R_{lm}(r) = A_{lm} S_{lm}(r) \quad \textit{with the abbrevations}$$

$$S_{lm}(r) = \left[J_m\left(a_{ml} \frac{r}{r_i}\right) - \frac{\dfrac{\partial J_m(a_{ml})}{\partial r}}{\dfrac{\partial Y_m(a_{ml})}{\partial r}} Y_m\left(a_{ml} \frac{r}{r_i}\right) \right] \quad \textit{and}$$

$$A_{lm} = \left\{ \frac{1}{2} r_a^2 \left[1 - \left(\frac{m}{a_{ml} \dfrac{r_a}{r_i}} \right)^2 \right] S_{lm}^2\left(a_{ml} \frac{r_a}{r_i}\right) - \frac{1}{2} r_i^2 \left[1 - \left(\frac{m}{a_{ml}} \right)^2 \right] S_{lm}^2(a_{ml}) \right\}^{-\frac{1}{2}},$$

$$\Psi_m(\varphi) = \frac{1}{\sqrt{2\pi}} e^{im\varphi}$$

(7.2)

J_m and Y_m denote the Bessel functions of the first and second kind and of order m. The eigenmodes are characterised by the three integers $N \equiv (nlm)$, with n representing the number of peaks in the axial, l their number in the radial, and m their number in the circumferential direction, respectively. Pure axial eigenmodes, e.g. have l=m=0 and n≠0. The a_{lm} are the infinite number of zeros of

$$\frac{\partial J_m(a_{lm})}{\partial r} \frac{\partial Y_m\left(a_{lm} \dfrac{r_a}{r_i}\right)}{\partial r} - \frac{\partial Y_m(a_{lm})}{\partial r} \frac{\partial J_m\left(a_{lm} \dfrac{r_a}{r_i}\right)}{\partial r} = 0$$

(8)

This equation ensures that the proper boundary condition $\partial\Phi/\partial n = 0$ is satisfied at $r=r_i$ and $r=r_a$. Note that due to the choice of the constants, the Φ_{nlm} are orthogonal and normalised: $(\Phi_{nlm}, \Phi_{n'l'm'}) = \delta_{nn'}\delta_{ll'}\delta_{mm'}$.

The corresponding eigenfrequencies ω_{nlm} are

$$\omega_{nlm} = c \sqrt{\left(n \frac{\pi}{L}\right)^2 + \left(\frac{a_{lm}}{r_i}\right)^2} \qquad (9)$$

approaching in the limit of a thin cylinder ($r_i \rightarrow r_a$) and for l≠0 /3/

$$\omega_{nlm} \rightarrow c\sqrt{\left(n\frac{\pi}{L}\right)^2+\left(\frac{\pi l r_a}{(r_a-r_i)r_i}+\frac{4m^2+3}{8\pi l r_i^2}(r_a-r_i)\right)^2}$$

Eigenmodes with circumferential contributions ($m\neq 0$) are two-fold degenerate, because for integer values of m the following relations hold :

$J_{-m} = (-1)^m J_m$ and $Y_{-m}=(-1)^m Y_m$

Hence, equation (8) depends only on m^2. This is an immediate consequence of the circumferential symmetry of the cylinder and remains valid also in the annular combustion chamber.

Note that the eigenvalues and -functions strongly depend on geometry and on the respective boundary conditions. If the wall is open at z=0 (p=0), for example, the only changes in the eigenfunctions and the eigenfrequencies in equations (7) and (9) are

$$Z_n(z) = \sqrt{\frac{2}{L}}\sin\left(\left\{n+\frac{1}{2}\right\}\frac{\pi}{L}z\right)$$
$$\omega_{nlm} = c\sqrt{\left(\left\{n+\frac{1}{2}\right\}\frac{\pi}{L}\right)^2+\left(\frac{a_{lm}}{r_i}\right)^2} \qquad (10)$$

A further aspect which might have an influence on the eigenmodes and which will be investigated later in the numerical examples, is a spatially distributed velocity of sound $c=c(r,\varphi,z)$ which is related to the local temperature and species in the combustion process. Consider as a typical example the cylinder where one half ($0 \le z \le L/2$) has $c(r,\varphi,z) = 2\,c_0$ and the other $c(r,\varphi,z) = c_0$ ($L/2 \le z \le L$). In this case an incoming longitudinal wave of type exp(ikz) is not only reflected at the end of the cylinder (z = L) but is also split half way down the cylinder (at z = L/2) into a transmitted and a reflected part. All these contributions superimpose to produce a standing wave in the entire cylinder. In this problem the eigenfrequencies are calculated assuming rigid walls across the entire boundary.

$$\omega_{nklm} = c\sqrt{\left(nf_k\frac{\pi}{L}\right)^2+\left(\frac{a_{lm}}{r_i}\right)^2} \qquad (11)$$

$with\ f_0 = 0.\ f_1 = 0.3661.\ f_2 = 0.6339 (k = 0.1.2)$

Note that additional eigenmodes in the z-direction arise whereas the modes in the radial and the circumferential directions are not affected.

3.2 Confirmation of the analytical results by FE analysis

For a validation of the FE tool, the eigenmodes as given in equations (7) to (10) for the cylindrical ring model of the combustion chamber have also been calculated numerically. The geometry parameters are chosen to represent the main dimensions of the annular combustion chamber. In Table 1 some of the eigenfrequencies including the related integers (nlm) and the ordering mode number N are presented. The entire boundary is assumed to be a rigid wall. The last three columns of the table include the analytical results (ω/ω_0 anal) for the eigenfrequencies evaluated from solving Equations. (7) and (8), the results of the FE analysis (ω/ω_0 FE) and the error of the numerical values compared to the analytical ones, respectively. The numerical analysis is performed with the ABAQUS code /4/ which iteratively extracts a certain number of eigenvalues closest to a prescribed shift frequency ω_s. The properties of the enclosed gas are characterised by its inverse compressibility 1/k and density ρ. As the frequencies are determined by the velocity of sound c only, it is convenient to take $\rho \equiv 1$ and $1/k = c^2$ (cf. equations 3, 8, 9).

By variation of ω_s and of the number of frequencies to be calculated the complete spectrum of eigenvalues is covered. For the lowest eigenvalues the ω_s is chosen negative resulting in $\omega_1=0$.

n	(n l m)	ω/ω_0 anal	ω/ω_0 FE	Error [%]
1	**0 0 0**	**0**	**0**	**0**
2	0 0 1	0,321	0,321	-0,005
3	0 0 1	0,321	0,321	-0,005
4	0 0 2	0,642	0,642	-0,002
5	0 0 2	0,642	0,642	-0,002
6	0 0 3	0,960	0,960	0,000
7	0 0 3	0,960	0,960	0,000
8	0 0 4	1,276	1,276	-0,002
9	0 0 4	1,276	1,276	-0,002
10	**1 0 0**	**1,342**	**1,343**	**-0,009**
11	1 0 1	1,380	1,380	-0,010
12	1 0 1	1,380	1,380	-0,010
13	1 0 2	1,488	1,488	-0,008
14	1 0 2	1,488	1,488	-0,008
15	0 0 5	1,588	1,588	-0,006
16	0 0 5	1,588	1,588	-0,006
17	1 0 3	1,650	1,650	-0,007
18	1 0 3	1,650	1,650	-0,007
19	1 0 4	1,852	1,852	-0,006
20	1 0 4	1,852	1,852	-0,006
21	0 0 6	1,896	1,897	-0,009
22	0 0 6	1,896	1,897	-0,011
23	1 0 5	2,079	2,080	-0,007
24	1 0 5	2,079	2,080	-0,007
25	0 0 7	2,200	2,201	-0,020
26	0 0 7	2,200	2,201	-0,018
27	1 0 6	2,323	2,324	-0,010
28	1 0 6	2,323	2,324	-0,010
29	**0 1 0**	**2,461**	**2,461**	**-0,011**
30	0 1 1	2,483	2,483	-0,010
...				
39	0 1 3	2,657	2,657	-0,010
40	**2 0 0**	**2,685**	**2,689**	**-0,160**
41	2 0 1	2,704	2,708	-0,158
...				
48	0 1 4	2,801	2,801	-0,010
49	**1 1 0**	**2,803**	**2,803**	**-0,011**
50	1 1 1	2,823	2,823	-0,011
...				
88	1 0 11	3,631	3,635	-0,096
89	1 0 11	3,631	3,635	-0,096
90	**2 1 0**	**3,642**	**3,645**	**-0,097**
91	2 1 1	3,657	3,660	-0,097
...				
119	**3 0 0**	**4,027**	**4,057**	**-0,742**
...				
183	**0 2 0**	**4,898**	**4,905**	**-0,159**
...				
250	0 2 7	5,411	5,469	-1,060

Table 1: Selected Eigenfrequencies of the cylinder model. The analytical solution is compared to the FE results. The bold typed frequencies indicate modes with axial/radial (no hoop) contributions only.

In order to increase the computational efficiency of the FE analysis, including either reducing the computation time or increasing the accuracy with a more refined mesh, only one quarter of the cylinder is modelled (cf. Fig. 3). The entire spectrum of eigenvalues is then obtained by splitting the calculation into two steps with different boundary conditions (BC). The first step imposes a rigid "wall" at both circumferentially directed boundaries (symmetrical BC). The second step assumes an open "wall" at one of these boundaries and a rigid "wall" at the other (asymmetrical BC). As a consequence, the aforementioned circumferential degeneracy is removed and every eigenfrequency is calculated only once. The "asymmetrical step" provides modes with circumferential contributions that are known to be two-fold degenerate. The "symmetrical step", however, provides all kinds of modes. Their degeneracy can be only assessed by considering the pressure distribution. The non-degenerate eigenmodes are readily revealed within the FE scheme by a third analysis with a 2D axisymmetric model providing the pure axial / radial modes (with $m \neq 0$) exclusively. In the case of the simple cylinder, it is not necessary to apply this procedure. However, it will be required for more complex domains such as realistic annular combustors.

The mesh used in the analysis of the cylinder ring consists of 375 isoparametric 20-node brick elements resulting in a total of 2076 pressure degrees of freedom. The agreement of numerical and analytical results is excellent, the maximum error is 1%. The discrepancy between analytical and numerical values increases with mode number N, as the spectrum gets denser. In principle, these errors can be further reduced with a more refined mesh, a properly chosen shift frequency and with increasing the number of iteration vectors in the analysis. Fig 2 depicts the complete spectrum of eigenfrequencies versus mode number N in the range $0<\omega/\omega_0<10$. The dashed line represents the limit curve in equation (4). Still higher frequencies ($N \geq 10^6$) must be used before the actual curve is smoothed out and approaches its limit.

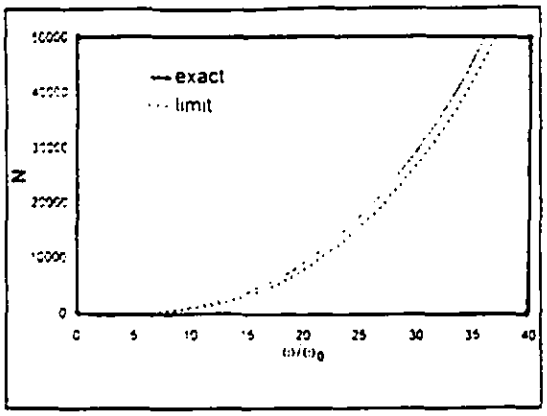

Figure 2: Eigenfrequency spectrum of the cylinder model. The limit curve is given by $N=(\omega/\omega_0)^3$ (see equation (4)).

In Fig. 3 two examples of a related pressure distribution are given: N=29, (nlm)=(010), ω/ω_0=2.461 and N=39, (nlm)=(013), ω/ω_0=2.657.

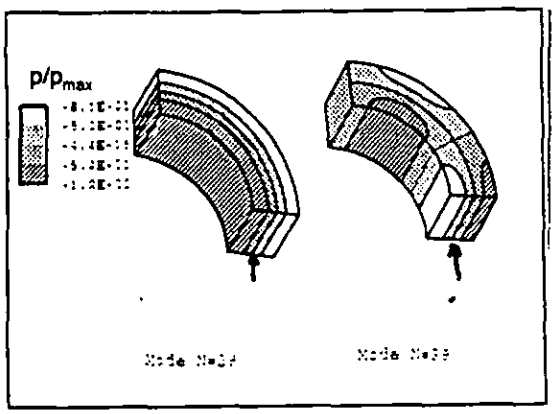

Figure 3: Examples of eigenmodes of the cylinder model: Mode N=29(left) and N=39(right).The eigenmodes are characterised by the normalised pressure distribution.

Note that the pressure values are normalised so that the maximum is 1. Mode 29 includes a standing wave with the shape of a sine function extending in radial direction. The set of nodes (p=0) is indicated by the arrows. It divides the original cylinder into two concentric parts of nearly equal thickness. The higher the numbers (nlm) the more peaks will occur in the eigensolution and the more complicated the set of nodes will be as indicated by mode 39 having one sine in the radial and three in the circumferential direction.

With a space dependent velocity of sound $c=c(\vec{x})$, similar results are obtained: In particular, the eigenfrequencies given by the analytical expression (9) are reproduced by FE analysis with the same high accuracy. The spatial dependence is technically taken into account by a prescribed temperature field T(x) with temperature dependent material parameters 1/k=1/k(T(x)).

In conclusion, FE analysis provides the complete eigenspectrum of acoustic wave motion with rather high precision, in particular, for the low frequencies that are sufficiently distinct. For circumferentially symmetric geometries, the efficiency of the calculation can be increased by making use of symmetry and by splitting the calculation into several independent steps with proper boundary conditions at the cut.

Most of these results remain valid for the more complex cone shaped geometry of the annular combustion chamber to be studied in the next chapter, of which an analytical solution is no longer available.

4 Eigenmodes of an inclined annular combustion chamber

In Fig 4 the geometry of an annular gasturbine combustor, typical for the Vx4.3A gas turbine family, together with the FE discretisation of a quarter of it is shown. The mesh consists of 4800 isoparametric 20-node brick elements including about 22400 degrees of freedom.

With this geometry fixed, the following types of analysis have been performed:

Analysis	I	II	III
velocity of sound	c_0=const	c=c(x) (see Fig 5)	c=c(x) (see Fig 5)
boundary condition at burner inlets	$\partial\Phi/\partial n$ =0 (rigid)	$\partial\Phi/\partial n$ =0 (rigid)	Φ =0 (open)

Rigid walls ($\partial\Phi/\partial n = 0$) are assumed at all other boundaries. The burner outlets are represented by 6 holes and the centres placed at equal distance in the middle of the surface adjacent to the burners.

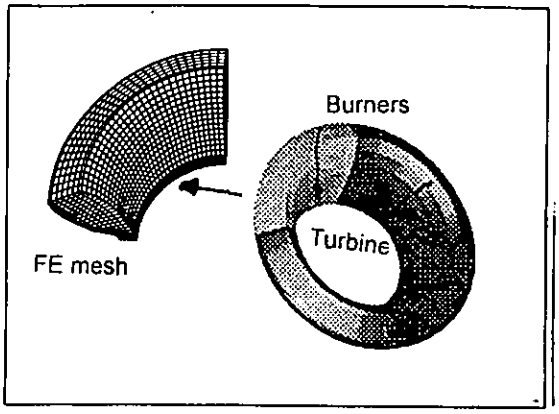

Figure 4: Geometry and FE model of the annular combustor

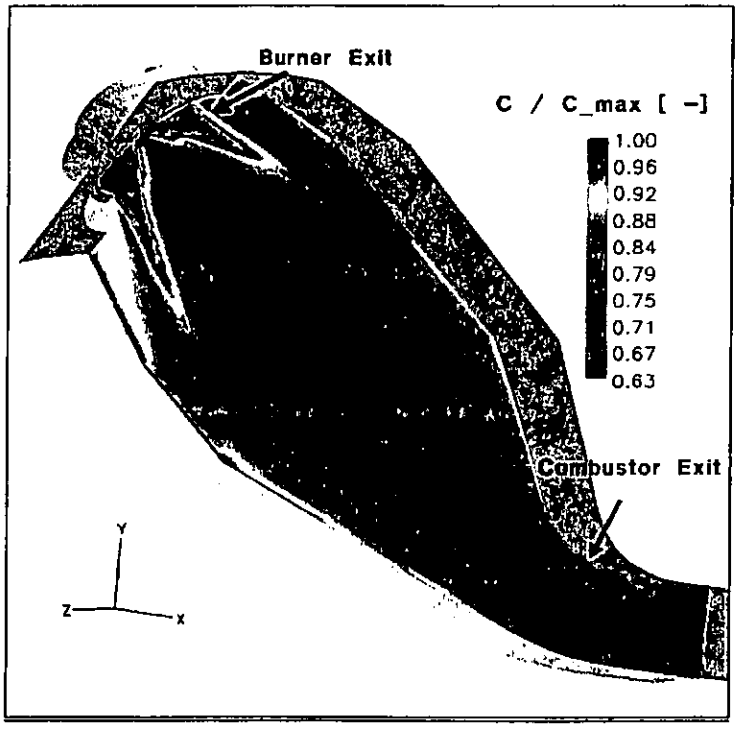

Figure 5: Distribution of the speed of sound normalised to its maximum value c_0 in the z=0 m plane (CFD calculation [7])

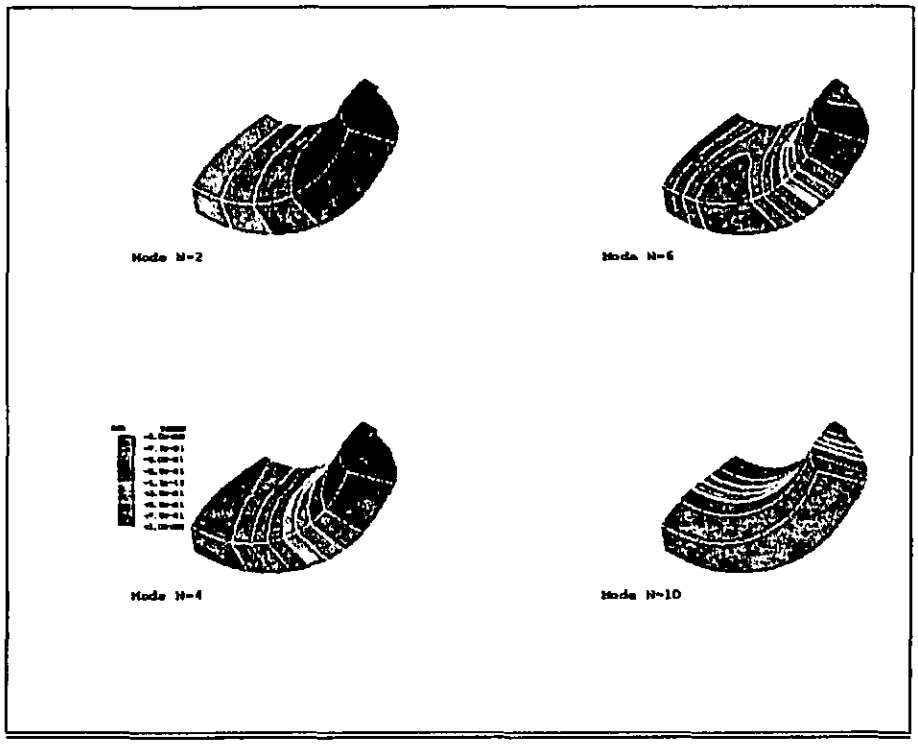

Figure 6: Selected eigenmodes of the annular combustor with boundary conditions of Problem II. The pictures show the normalised pressure distribution.

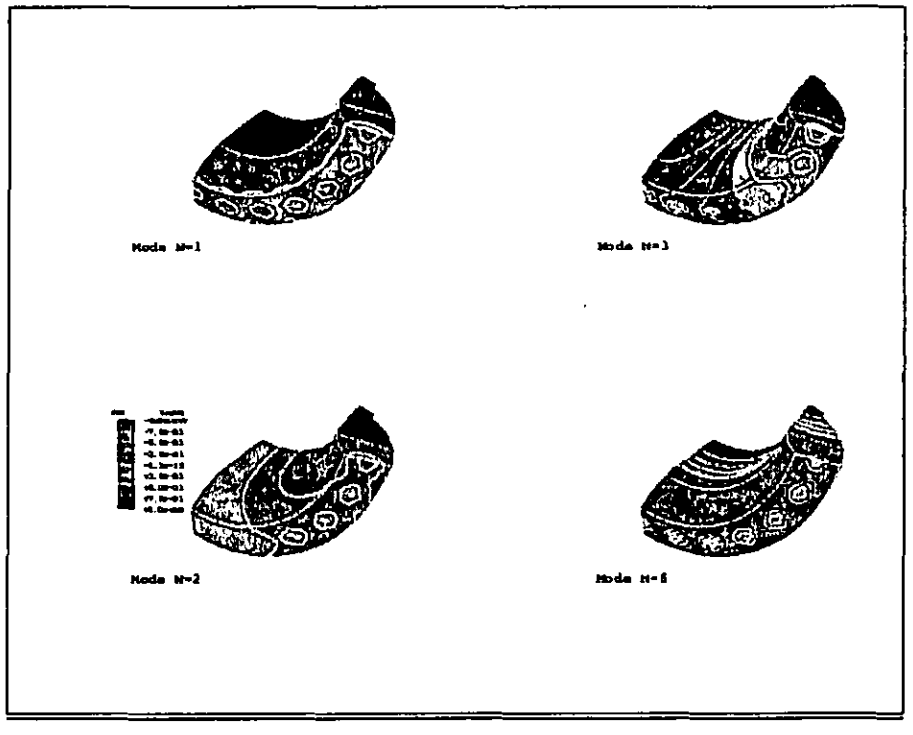

Figure 7: Selected eigenmodes of the annular combustor with boundary conditions of Problem III. The normalised pressure distribution is shown.

The spatial distribution of the velocity of sound $c(x)/c_0$ is given in Fig. 5. c_0 is the maximum speed of sound in the combustion chamber. c(x) is calculated from the temperature field and the distribution of

species concentration taken from a CFD analysis of the combustion process /3/. The distribution of the speed of sound c(x) is quite similar to the temperature distribution. It is nearly constant $c(x)=c_0$ downstream of the flame front which covers most of the combustion chamber. Values c(x) less than c_0 are observed upstream of the flame front in the immediate vicinity of the burner outlets and near the wall, where cooling air is added. In the inner recirculation zone, values greater than c_0 are calculated.

In Table 2 the eigenfrequencies for problems I, II and III are listed. The values are again normalised by $\omega_0 = c_0 (6\pi^2/ V)^{1/3}$. As before, the non-degenerate modes are marked as bold characters. To avoid repetitions, the degenerate modes are mentioned only once, resulting in steps of 2 of the mode number N in the list. For comparison the cylinder solution of the preceding section with rigid walls assumed at all boundaries is also given.

(N_i)	Problem I	Problem II	Problem III	Problem IV
1	**0**	**0**	**0.56**	**0**
2	0.32	0.32	0.65	0.32
4	0.63	0.63	0.87	0.64
6	0.94	0.93	1.14	0.96
8	1.24	1.22	1.42	1.28
10	**1.35**	**1.34**	**1.53**	**1.34**
11	1.39	1.38	1.57	1.38
13	1.53	1.51	1.68	1.49
15	1.53	1.52	1.70	1.59
17	1.72	1.72	1.86	1.65
19	1.81	1.78	1.98	1.85
21	1.97	1.96	2.09	1.90
23	2.09	2.05	2.24	2.08
25	2.24	2.24	2.35	2.20
27	**2.34**	2.31	**2.36**	2.32
28	2.36	**2.31**	2.37	**2.46**
30	2.36	2.33	2.43	2.48
32	**2.41**	**2.37**	**2.48**	2.50
33	2.43	2.39	2.50	2.55
35	2.43	2.39	2.51	2.58
37	2.49	2.46	2.52	2.66
39	2.52	2.48	2.58	**2.68**
41	**2.54**	2.52	2.62	2.70
43	2.60	2.56	2.63	2.76
45	2.63	2.59	2.70	2.79
47	2.67	2.60	2.76	**2.80**
49	2.77	2.75	2.78	2.80
51	2.81	2.76	2.86	2.82
53	2.82	2.81	2.90	2.84
55	2.89	2.82	2.94	2.85
57	2.97	2.91	3.01	2.88
59	3.00	2.97	3.06	2.97
61	3.10	3.06	3.12	2.98
63	3.15	3.09	3.18	2.98
65	3.19	3.09	**3.23**	3.09
67	3.20	**3.20**	3.24	3.10
69	**3.26**	3.21	3.25	3.11
70	3.28	3.21	3.25	3.11
72	3.33	3.26	3.29	3.18
74	3.38	3.28	3.32	3.27
76	3.40	3.29	3.36	**3.29**
78	3.40	3.34	3.45	3.37
80	3.41	3.36	3.47	3.37
82	**3.43**	**3.41**	**3.54**	3.41
83	3.45	3.43	3.54	3.45
85	3.47	3.44	3.55	**3.47**
87	3.50	3.47	3.55	3.63
89	3.51	3.48	3.58	**3.64**
91	3.58	3.51	3.60	3.66
93	3.62	3.56	3.60	3.66
95	3.64	3.56	3.68	3.66
97	3.65	3.57	3.69	3.67
99	3.66	3.61	3.75	**3.67**
101	3.69	3.68	3.75	3.70
103	3.75	3.73	3.79	3.78
105	3.80	3.75	3.79	3.88
107	3.83	3.76	3.82	3.88
109	3.86	3.81	3.92	3.90
111	3.91	3.82	3.93	3.90
113	3.92	3.84	3.93	3.93
115	3.98	3.90	4.00	3.94
117	4.00	3.99	4.06	4.01
119	4.04	4.00	4.09	4.03
121	4.10	4.02	4.10	4.04
123	4.17	4.03	4.12	4.08
125	4.17	4.07	4.14	4.09
127	4.17	4.10	4.24	4.14
129	4.19	4.18	**4.25**	4.15
131	**4.27**	**4.22**	4.26	4.16
132	4.29	4.23	4.28	4.16
134	4.32	4.24	4.30	4.21
136	4.33	4.27	4.33	4.22
138	4.35	4.28	4.34	4.22
140	4.39	4.31	4.36	4.31
142	4.39	4.31	4.39	4.33
144	4.40	4.33	4.41	4.34
146	4.42	4.35	4.44	4.41
148	4.43	4.40	4.44	4.43
150	4.47	**4.42**	4.52	4.45
152	**4.50**	4.42	4.55	4.49
153	4.51	4.43	4.56	4.50
155	4.55	4.46	4.58	4.54
157	4.58	4.51	**4.59**	**4.54**
159	4.61	4.52	4.61	4.59

Table 2: Eigenfrequencies of an annular gasturbine combustion chamber according to problems I, II, and III (see text), and, for comparison, to the cylinder model of Chapter 3. The bold typed frequencies indicate modes with axial/radial (no hoop) contributions only.

As the annular combustion chamber has the

shape of a cone, the axial and radial directions mix and the integers (nl) have no meaning anymore. Nevertheless, the low eigenfrequencies $\omega < 2\omega_0$ for Problems I, II, and the cylinder model are in good agreement and show distinct gaps. For higher values of ω/ω_0 the eigenfrequencies become blurred, and minor differences in the mode shape occur in these three problems. For example the third axial/radial mode is assigned to N=27 in Problem I and the cylinder problem, but it is assigned to N=28 in Problem II. Hence, in Table 2 the numbers N only refer to Problem I. The effect of the space dependent velocity of sound c(x) in Fig.5 is about 5% for the entire spectrum. In Fig 6 four examples of pressure distributions corresponding to problem II are shown. The locations of pressure nodes are indicated by the interface areas between the two green colours. Modes 2 and 4 are the lowest circumferential dominated modes, mode 10 is the lowest mode without any circumferential contribution. Mode 6 is a typical mixed mode.

Problems I, II and the cylinder problem have equally formulated boundary conditions of Neumann type on all boundaries, whereas for Problem III at the circular holes of the burner inlets a Dirichlet type boundary condition has been prescribed. Hence, the lowest eigenfrequency is greater than zero and the spectrum is completely different to the other three, as already becomes evident looking at formulas (9) and (10). Fig. 7 confirms this showing some simpler mode shapes. The lowest eigenfrequency corresponds to a half-sine primarily in axial direction. Mode 2 and 3 are the lowest modes showing distinct circumferential contributions. Mode 6 has dominant axial-/radial contributions and corresponds to mode 10 in the preceding example.

5 Conclusion

An analysis of the acoustic wave motion of an annular gasturbine combustor has been performed.

The quality of the analysis has been verified using a cylinder ring, which is a simple geometry with an analytical solution. It is demonstrated that the entire acoustic spectrum can be calculated by FE analysis with rather high accuracy for the lower frequencies that are sufficiently far apart from each other. The efficiency of the numerical eigenvalue analysis can be improved by making use of symmetry, by splitting the problem into several steps with alternate boundary conditions, and by choosing the shift frequency ω_s in the range of frequencies one is interested in. An inhomogeneous velocity of sound has been included.

The 200 lowest eigenmodes of an annular combustion chamber are calculated by FE analysis within a quarter section model. The analysis also provides a normalised pressure distribution identifying the set of nodes of the respective modes. At the burner side different boundary conditions have been imposed. It is demonstrated that this has a strong influence on the eigen frequency spectrum. Therefore, it is inevitable to know the burner impedance precisely. Since no mixing air is added to the combustion system, the effect of a space dependent velocity of sound on the spectrum is only about 5%. As observed in every kind of cavity, the eigenfrequency spectrum shows distinct gaps for the lower modes, whereas the higher modes, which have been given to show the quality of the FE scheme and the role of the boundary conditions, become blurred.

References

[1] Becker, B., Schulenberg, T., Termuehlen, H.: The 3A-series gas turbines with HBR™ combustors, ASME Paper 95-GT 458, 1995

[2] Samaniego, J. M., Yip, B., Poinsot, T., Candel, S., "Low frequency combustion instability mechanism in a side-dump combustor, Combustion and Flame, Vol. 94, pp. 363-380, 1993.

[3] Paschereit, C. O., Polifke, W., "Investigation of the thermoacoustic characteristics of a lean premixed gas turbine burner", ASME Paper 98-GT-582, 1998

[4] Prade, B., Streb, H., Berenbrinck, P., Schetter, B., Pyka, G., "Development of an improved hybrid burner - initial operating experience in a gas turbine", ASME Paper 96-GT-45.

[5] P. M. Morse, K. U. Ingard: Theoretical Acoustics. Princeton University Press 1986.

[6] Hibbitt, Karlson & Sorenson, Inc. ABAQUS User's Manual Version 5.7. 1997.

[7] W. Krebs, G. Walz, S. Hoffmann, H. Judith : Detailed analysis of the thermal wall heat load in annular combustors, submitted for presentation at the ASME TURBO EXPO 1999